

CHAPTER 1. INTRODUCTION

X-ray binaries are among the brightest of X-ray sources in the sky with SCO X-1 being the brightest of them. It was the first X-ray source discovered by an Aerobee rocket carrying a payload consisting of three large area Gieger counter (Giacconi et. al. 1962). Later in 1970, *Uhuru* the first satellite dedicated to X-ray astronomy was launched (Kellogg 1975). Now more than three decades after the first dedicated X-ray astronomy satellite and with many other X-ray missions, X-ray astronomy has changed our view of the universe. It has revealed to us a universe which witnesses various explosive and high energy phenomena. Various objects emit X-rays by different mechanisms, e.g., some rotation-powered pulsars emit X-rays by synchrotron radiation, supernova remnants emit X-rays due to thermal bremsstrahlung, atomic lines and from shocks as the ejecta collides and sweeps up the interstellar medium, etc. The most variable sources like the Active Galactic Nuclei (AGNs) and the X-ray binaries are powered by accretion of matter onto compact objects. In this work we have studied various aspects of X-ray binaries that contain high magnetic neutron stars. The first part of the thesis concentrates on the orbital evolution and apsidal motion measurements in a few X-ray binary pulsars and the second part consists of the study of long term variabilities in the intensity of X-ray binaries. We have used Rossi X-ray Timing Experiment (RXTE) data for the work presented in the thesis. RXTE is briefly described in the last section of this chapter.

1.1 X-ray Binaries

X-ray binaries are systems consisting of a compact object which is gravitationally bound to a normal companion star. The compact object can be either a neutron star or a black hole candidate. In this thesis, companion star always refers to the normal star unless otherwise

mentioned.

X-ray binaries are all powered by accretion of matter on to the compact star. The companion star donates matter to the compact star either via Roche lobe overflow or by stellar wind outflows. If a compact star of mass M_* and radius R_* accretes matter at the rate of \dot{M}_* , then the accretion luminosity is given by

$$L_{acc} = \frac{GM_*\dot{M}_*}{R_*} \quad (1.1)$$

assuming all the kinetic energy of infalling material is converted to radiation. The above relation is true for spherical accretion and clearly shows that the accretion luminosity is dependant on the compactness (i.e, M_*/R_*) of the accretor. Thus the accretion yield for a main sequence star is much smaller than that, say, for a neutron star. For any accretor there is also a maximum luminosity that can be generated via spherical accretion. This is called Eddington luminosity (L_{edd}) and is a good order of magnitude estimate even when the spherical accretion assumption is not true. L_{edd} can be estimated by equating outward radiation pressure and gravitational force on an electron proton pair.

$$L_{edd} = \frac{4\pi GMm_p c}{\sigma_T} \quad (1.2)$$

where m_p is the mass of a proton and σ_T is the Thomson scattering cross-section. Thus every object of mass M has a limiting luminosity which it cannot exceed.

An accretion disc is formed around the compact object whenever the specific angular momentum J of the infalling matter is too large for direct impact onto the stellar surface. We define the circularisation radius as $R_{circ} = J^2/GM$, which is where the matter would orbit with constant angular momentum. A disc is formed only when R_{circ} is greater than the effective size (R_{eff}) of the accretor. For a non-magnetic neutron star R_{eff} is its radius whereas for a magnetised neutron star R_{eff} is radius of its magnetosphere. For a black hole R_{eff} is the radius of the last stable circular orbit. The infalling matter has to lose its angular momentum before it is finally accreted by the compact object. Viscosity is responsible to transport all

the angular momentum outwards, allowing most of the matter to be transported to the inner regions of the disk while only a very small fraction of matter is used to carry away most of the angular momentum. As the matter moves through the accretion disk, approximately half of its potential energy is radiated away. The wavelength of the observed radiation is determined by the position of the radiating matter in the disk. In the outer disk the temperatures are of the order of a few thousand degrees and therefore the radiation will be in the IR and optical band. In the inner regions of the disk the temperatures can reach several million degrees producing UV and X-ray emission.

When the compact object is a neutron star with a high magnetic field, the accretion flow pattern close to the stellar surface is determined by its magnetic field. Whether the accreting material gets accreted onto the compact object or is propelled away is determined by the interaction of spin period of neutron star and the Keplerian frequency of the infalling matter at the Alfvén radius which is defined as the radius at which magnetic pressure of the neutron star becomes equal to the ram pressure of the infalling matter (Frank, King & Raine 1992).

$$r_A = 5.1 \times 10^8 \dot{M}_{16}^{-2/7} M_1^{-1/7} \mu_{30}^{4/7} \text{ cm} \quad (1.3)$$

In the above equation \dot{M}_{16} is mass accretion rate in the units of 10^{16} g s^{-1} , M_1 is mass of the neutron star in units of $1 M_\odot$ and μ_{30} is magnetic moment of the neutron star in units of 10^{30} G cm^3 . If the stellar spin frequency is greater than the Keplerian frequency of orbiting matter at Alfvén radius, then the accreting material is blown away as the matter can not overcome the centrifugal barrier to get accreted onto the neutron star. This is called the propeller regime because the matter eventually escapes the neutron star in the form of wind and no pulsations are seen from the X-ray pulsar. If the stellar spin frequency is smaller than the orbital frequency of matter at the interaction radius, the accreting material is forced into corotation with the star and is channelled along the field lines onto the magnetic poles. The gravitational energy of the infalling matter is emitted as X-rays from the magnetic poles. If the optical depth of the accretion column is low, the radiation is emitted along the magnetic axis forming a pencil beam whereas if the optical depth is high, radiation escapes tangential to

the accretion column forming a fan beam. Whenever this rotating beam of radiation is aligned to our line of sight, we receive a pulse of radiation. Due to regular reception of such pulses these objects are also called pulsars. It is observed that X-ray pulsars spin-up or spin-down due to variable mass accretion rate. The spin-up or spin-down of the neutron star depends on the sense of the net angular momentum of the accretion process with respect to the spin of the neutron star. When the net angular momentum has the same sense as that of the neutron star's spin, neutron star is spun up whereas when the sense is opposite, neutron star is spun down.

Depending on the mass of the companion star, X-ray binaries are broadly classified into two types; High mass X-ray Binaries (HMXBs, $M_{comp} \geq 10M_{\odot}$) and Low mass X-ray Binaries (LMXBs, $M_{comp} \leq 1M_{\odot}$).

There are more than 200 known HMXBs and 25 of them have well measured orbital parameters. There are mainly two types of HMXBs. Strong persistent systems with $P_{orb} \leq 10$ days and $e \leq 0.1$ (eg. Cen X-3, SMC X-1, Cyg X-1, etc) and transient systems having wide eccentric orbits of $P_{orb} \sim 20 - 100$ days and $e \sim 0.3 - 0.5$. HMXBs have hard X-ray spectra with $kT \geq 15$ keV. X-ray spectra of HMXB pulsars show cyclotron lines due to the high magnetic field ($B \sim 5 \times 10^{12}$ G) of the neutron stars. They are generally located in the Galactic plane and are believed to be young systems ($age < 10^7$ yr). Persistent sources generally have O-type companions with strong stellar wind, almost filling their critical Roche lobe. The neutron star accretes matter from the stellar wind of the companion star due to which it is a persistent X-ray source. Transient systems have Be-star companions which are fast rotators and have sudden outbursts during which mass is ejected from the star along the equator in a stellar disk. During these episodes of mass ejection the compact star accretes matter and becomes X-ray bright.

LMXBs have orbital periods in the range of 11 min to 17 days. Due to a small companion star, generally the observed optical spectrum is that of the hot accretion disk. Except for a few cases neutron star in these systems generally have weak magnetic fields $\sim 10^9 - 10^{11}$ G and hence do not show X-ray pulsations. Instead they exhibit sudden X-ray bursts due to

thermonuclear fusion of accreted matter at the surface of the neutron star. These X-ray bursts are supposed to be suppressed if the magnetic field strength is greater than 10^{11} G (Lewin & Joss 1983) which explains why no bursts are generally observed in HMXB pulsars. There are at least a dozen LMXBs in which the compact object is most probably a black hole. LMXBs have soft X-ray spectra ($kT \sim 2$ keV). In these systems accretion is via Roche lobe overflow. These systems are generally found near the Galactic center and in Globular clusters which implies these are older systems (age $> 10^9$ yr).

It is natural to expect that there must be systems with companion stars with masses between $1M_{\odot}$ and $10M_{\odot}$ which can be called Intermediate Mass X-ray Binaries (IMXBs). But these systems are not easily observed due to a simple selection effect which can be understood as follows (Tauris & van den Heuvel 2006). HMXBs have evolved giant companions that are massive enough to have a strong stellar wind mass-loss-rate. This would be sufficient to power the compact object for $10^5 - 10^6$ years making it a bright X-ray source. On the other hand LMXBs are powered by accretion via Roche-lobe overflow. LMXBs evolve slowly on a nuclear timescale of $10^8 - 10^9$ years. In IMXBs the companion star are not massive enough to produce sufficiently high wind mass-loss rates to power an observable X-ray source. Subsequently when IMXBs evolve through Roche-lobe overflow, the relatively large mass ratio between the companion star and the neutron star makes the timescale of evolution only about a few 1000 yr. Furthermore, the very high mass-transfer rates under these circumstances ($\dot{M} > 10^{-4}M_{\odot} \gg \dot{M}_{Edd}$) may cause the emitted X-rays to be absorbed in the dense gas surrounding the accreting neutron star. Thus it is naturally evident that it is very difficult to observe an IMXB. A few IMXBs which have been observed are Her X-1 ($M_c 3.0M_{\odot}$), GRO J1655-40 ($M_c 1.5M_{\odot}$), 4U1543-47 ($M_c 2.5M_{\odot}$), LMC X-3 ($M_c 5.0M_{\odot}$) and V 4642 Sgr ($M_c 6.5M_{\odot}$).

1.2 Binary Orbit of the neutron star

Pulses from the neutron star as recorded by an observer are advanced or delayed according to the position of the neutron star in its orbit. When the neutron star is moving towards the

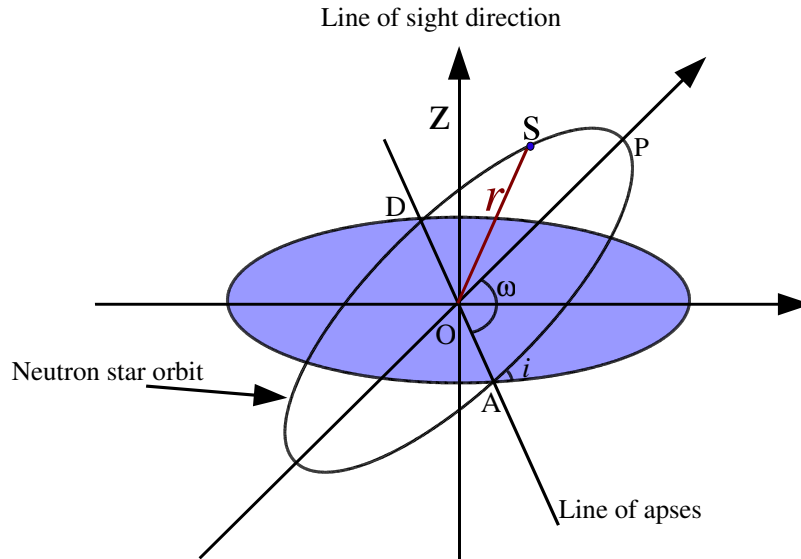


Figure 1.1 Figure represents the neutron star orbit. The line of sight direction is z and S is the position of the neutron star in the orbit at any time t

observer, the pulses arrive faster and when the neutron star is moving away from the observer, the pulses are delayed. Using this fact we can determine the orbit of the neutron star. The details of this analysis will be explained in the coming chapters. Here we detail the different orbital elements which describe the neutron star orbit. Figure 3.1 illustrates the neutron star orbit with respect to the plane perpendicular to the line of sight of the observer. The angle i is called the inclination angle and is the angle between the plane containing the neutron star orbit and the plane perpendicular to the line of sight. Point A in the Figure is the ascending node and the plane perpendicular to the line of sight. Point A in the Figure is the ascending node and point D is the descending node. The line joining the ascending node and the descending node is called the *line of apses*. Point P is the periastron point or the point of nearest approach between the neutron star and the companion star. The angle between the line joining the center of the orbit to the periastron point and the line of apses is called the angle of periastron and is denoted by ω . the time when the neutron star crosses the periastron point is called the time of periastron passage and is denoted by T_ω . The time taken by the neutron star to complete one orbit is called the orbital period and is denoted by P_{orb} . The position (S)

of the neutron star in its orbit, depends on time t implicitly through the dependence of mean anomaly (M) on time and, is given by

$$r = \frac{a_x(1 - e^2)}{1 + e \cos \nu} \quad (1.4)$$

where e is the eccentricity of the neutron star orbit and ν is the eccentric anomaly of the orbit. ν is related to the mean anomaly M and hence P_{orb} as

$$\tan\left(\frac{\nu}{2}\right) = \sqrt{\frac{1+e}{1-e}} \tan\left(\frac{E}{2}\right) \quad (1.5)$$

$$M = \frac{2\pi}{P_{orb}}t = E - e \sin E \quad (1.6)$$

Using the arrival time delay of the pulses from the neutron star we can measure the orbit of the neutron star projected on the line of sight axis (z). Therefore z is given by,

$$\begin{aligned} z &= r \sin(\nu + \omega) \sin i \\ &= \left(\frac{a_x \sin i (1 - e^2)}{1 + e \cos \nu} \right) \sin(\nu + \omega) \end{aligned} \quad (1.7)$$

Thus the orbit of the neutron star is completely determined by measuring the orbital elements described above. The evolution of the binary orbit can be seen by comparing the orbit measured at different epochs of time. Binary orbit can evolve due to mass transfer between the two stars, mass loss from the binary system, tidal interaction between the two stars and due to gravitational wave radiation. The effect of gravitational wave radiation on the evolution of the HMXB orbit is very small and cannot be detected with the present day accuracy of our observations. Therefore we do not discuss it further. The next section describes the binary orbit evolution due to above mentioned factors in detail.

1.3 Orbital evolution in X-ray binary pulsars

Orbital evolution mechanisms in X-ray binaries has been studied extensively (Zahn 1966 and 1975, Wheeler, Lecar and McKee 1975, Lecar, Wheeler and McKee 1976, Kelly et al. 1983). Below we give a brief description of orbital evolution of X-ray binary pulsars. The orbit of an X-ray binary is expected to evolve due to

1. Mass loss from the system due to stellar winds (eg. in O stars) or sudden mass ejections (eg. Be-stars)
2. Mass transfer from the companion star to the neutron star by Roche lobe over flow (eg. LMXBs) or by stellar wind capture (eg. HMXBs)
3. Tidal interaction between the neutron star and the companion star.

If M_c is mass of the companion star and M_x is mass of the neutron star then the orbital angular momentum Ω_c of the companion star and Ω_x of the neutron star are related by

$$\Omega_x = \Omega_c \left(\frac{M_c}{M_x} \right) \quad (1.8)$$

The total orbital angular momentum is given by $\Omega_T = \Omega_x + \Omega_c$. Let us denote mass ratio of the two stars by $q (= M_x/M_c)$ and the fraction of mass lost by M_c that is captured by M_x by $\beta (= -\dot{M}_x/\dot{M}_c)$. Then the rate of change of orbital angular momentum of the neutron star due to mass transfer and mass loss is given by

$$\begin{aligned} \dot{\Omega}_x &= \dot{\Omega}_c \left(\frac{M_c}{M_x} \right) + \Omega_c \left(\frac{\dot{M}_c}{M_x} \right) - \Omega_c \left(\frac{M_c}{M_x^2} \dot{M}_x \right) \\ &= \frac{\dot{\Omega}_T - \dot{\Omega}_x}{q} + \Omega_c \frac{\dot{M}_c}{M_c} \left(\frac{1}{q} + \frac{\beta}{q^2} \right) \\ &= \Omega_x \frac{\dot{M}_c}{M_c} \left(\frac{1 + \beta/q}{1 + q} \right) + \dot{\Omega}_T \left(\frac{1}{1 + q} \right) \end{aligned} \quad (1.9)$$

The first term in equation 1.9 gives the torque on the neutron star due to mass transfer and the second term represents the torque on the neutron star due to mass and angular momentum loss from the system. If the mass transfer is conservative in both total mass and angular

momentum, then $\beta = 1$ and $\dot{\Omega}_T = 0$. For non-conservative mass transfer, the rate of loss of total angular momentum is given by

$$\dot{\Omega}_T = \xi \dot{M}_T a_c^2 \omega_K = \xi \dot{M}_c (1 - \beta) a_c^2 \omega_K \quad (1.10)$$

where ξ is a dimensionless parameter that denotes the orbital angular momentum carried away per unit mass lost from the system, M_T is total mass of the system $M_T = M_x + M_c$, ω_K is the orbital angular velocity and a_c is the semi-major axis of the orbit of the companion star. Using equations 1.9 and 1.10 we get the total torque on the neutron star due to mass loss and transfer by $N_{\dot{m}} = \dot{\Omega}_x$,

$$N_{\dot{m}} = \dot{M}_c a^2 \omega_K \left(\frac{[1 + \beta/q + \xi(1 - \beta)]q^2}{(1 + q)^3} \right) \quad (1.11)$$

The gravitational pull of the neutron star produces tides on the companion star. These tides lag by an angle called tidal lag angle which is approximately proportional to the difference in angular velocity between the companion star and the orbit (Lecar, Wheeler & Mckee 1976; Zahn 1977; Kelley et al. 1983). If ω_c is the angular velocity and I_c is the moment of inertia of the companion star then the tidal torque on the neutron star N_t is given by

$$N_t = -I_c \frac{(\omega_K - \omega_c)}{\tau} \quad (1.12)$$

where τ is the synchronization time scale. Zahn (1977) showed that for radiatively damped dynamical tides the synchronization time is also a function of $\omega_K - \omega_c$. Thus the total torque on the neutron star due to mass transfer, mass loss and tidal interaction is given by

$$N = N_{\dot{m}} + N_t \quad (1.13)$$

From the total torque N on the neutron star we can estimate the instantaneous rate of change of orbital period P_{orb} as

$$\frac{\dot{P}_{orb}}{P_{orb}} = 3f \frac{\dot{M}_c}{M_c} - 3g \left(\frac{\omega_K - \omega_c}{\omega_K} \right) \frac{1}{\tau} \quad (1.14)$$

where

$$f = \frac{\beta}{q} - \frac{2/3 + \beta/3 + q[1 - \xi(1 - \beta)]}{1 + q} \quad (1.15)$$

$$g = \left(\frac{I_c}{M_c R_c^2} \right) \frac{(1 + q)^2}{q} \left(\frac{R_c}{a} \right)^2 \quad (1.16)$$

Apart from affecting the orbital evolution the tidal force exerted by the neutron star on the companion star also deforms the companion star. The rotation of the companion star will flatten the star at the poles and cause it to bulge at its equator. Both these factors thus change the mass distribution in the companion star and it is no longer spherical. This departure from spherical symmetry perturbs the binary orbit and causes it to precess. This precession of the binary orbit will slowly rotate the line of apses. The rotation of the line of apses then gives rise to rate of change of the angle of periastron(i.e, $\dot{\omega}$). Thus this precession of the orbit is called apsidal motion and measuring $\dot{\omega}$ allows us to quantify it. Since the rate of precession of the orbit is dependant on the mass distribution in the companion star, apsidal motion is directly proportional to the apsidal motion constant (k) of the companion star. Therefore measuring $\dot{\omega}$ allows us to test the stellar structure models by comparing the observed k and its theoretically predicted value.

1.4 Orbit Circularisation

A neutron star is born after supernova explosion. When such an explosion happens in a binary system, large amount of mass is lost from the system and the explosion itself will impart a radial impulse to the companion star (Wheeler, Lecar, and McKee 1975). These effects increase the semi major axis and the eccentricity of the orbit. But some HMXBs like Cen X-3, Her X-1, SMC X-1 have nearly circular orbits. Tidal interaction between the neutron star and the companion star tends to circularise the binary orbit. A detailed theory of orbit circularisation was developed by Zahn (1966), Alexander (1973) and more recent authors. The description we present here is the simplified version of this tidal dissipation (Lecar, Wheeler

and McKee 1976).

The neutron star raises a tide on the massive companion star. Dissipative processes in the companion star cause the tidal bulge to be non collinear with the centers of the two stars. Therefore the tidal bulge will lag or lead depending on whether the instantaneous orbital angular velocity is faster or slower than the spin angular velocity of the companion star. When the tidal bulge lags, it exerts a torque on the neutron star in a direction opposite to its orbital motion, tending to reduce its orbital angular momentum. The companion responds to this torque by spinning faster. The effects of a non collinear tidal bulge on the orbital elements varies with the orbital phase. If the tidal bulge lags at periastron, the instantaneous effect is to reduce both the eccentricity and the semi major axis. Lecar, Wheeler and McKee (1976), showed that the torque due to this tidal bulge varies as the inverse sixth power of the distance between the two stars. Therefore the effect of tidal dissipation is concentrated at periastron and to circularise the orbit it is required that the tidal bulge lag at periastron. The same tidal dissipative forces also synchronise the orbit. We note here that, Counselman (1973), showed that after the orbit has been circularised and synchronised, a subsequent decrease in semi major axis will start a continuing spiraling-in of the neutron star unless $M_x a^2 > 3I$, where I is the moment of inertia of the companion star.

1.5 Accretion disk precession in X-ray Binaries

X-ray binaries show periodic and/or quasi periodic time variability in the observed X-ray flux due to many reasons. Periodic variations are seen due to spin and orbital motion of neutron star. Quasi Periodic Oscillations (QPOs) of a few millihertz to a few kilohertz are seen due to material inhomogeneity orbiting the neutron star which blocks the X-rays in the line of sight of the observer. They also show periodic or quasi periodic time variabilities in observed X-ray flux at times scales greater than the respective orbital period of the binary due to changing mass accretion rate or due to a precessing accretion disk which is blocks the central X-ray source from the line of sight of the observer. These long term variations are termed as superorbital variations. Her X-1, LMC X-4, 2S 0114+650, show periodic superorbital variations

whereas SMC X-1, GRS 1747-312, Cyg X-2, etc. show quasi periodic superorbital variations in observed X-ray flux due to a precessing accretion disk. Theoretical models have shown that a tilted accretion disk about the neutron star will precess due to the tidal interaction with companion star. Numerical simulations of tilted, warped accretion disks illuminated by bright central X-ray source have resulted in quasi periodic and aperiodic precession of the accretion disks. Detailed discussion of these models is given in chapter 4 of the thesis where we present our work of the study of aperiodic X-ray flux variations in Cen X-3.

1.6 Rossi X-ray Timing Explorer

Rossi X-ray Timing Explorer (RXTE) is a space based X-ray detector that is in a low-Earth circular orbit at an altitude of 580 km with an orbital period of about 90 minutes with an inclination of 23 degrees. It was launched on December 30, 1995. It carries two pointed instruments, the Proportional Counter Array (PCA) which covers the lower energy range from 2 to 60 keV, and the High Energy X-ray Timing Experiment (HEXTE) which covers the upper energy range from 15 to 250 keV. A collimator is used to provide a FWHM field of view of 1 degree for both the pointed instruments. In addition to these two instruments, RXTE also carries an All-Sky Monitor (ASM) which scans about 80% of the sky every orbit and allows us to monitor the bright and transient X-ray sources at time scales of 90 minutes or longer. The instrument details provided below have been collected from the HEASARC website for RXTE.

1.6.1 Proportional Counter Array

PCA is made of 5 proportional counter units (PCU) and has a total photon collecting area of 6500 square cm. Figure 1.2 and 1.3 show the PCA assembly and one proportional counter of the PCA respectively. It has an energy resolution of about 18% at 6 keV and a very fine time resolution of 1 microsecond. The moderate spectral resolution also allows one to do spectral studies. PCA can detect a source of 0.1 mCrab with five sigma confidence level by observing it for 350 seconds. Its background count rate equivalent to 2 mCrab.

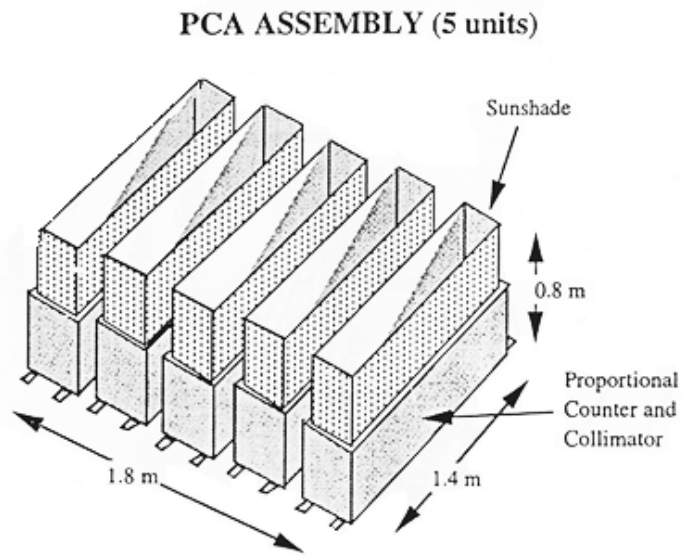


Figure 1.2 This Figure shows the PCA assembly of 5 proportional counters. Figure reproduced from NASA website for RXTE

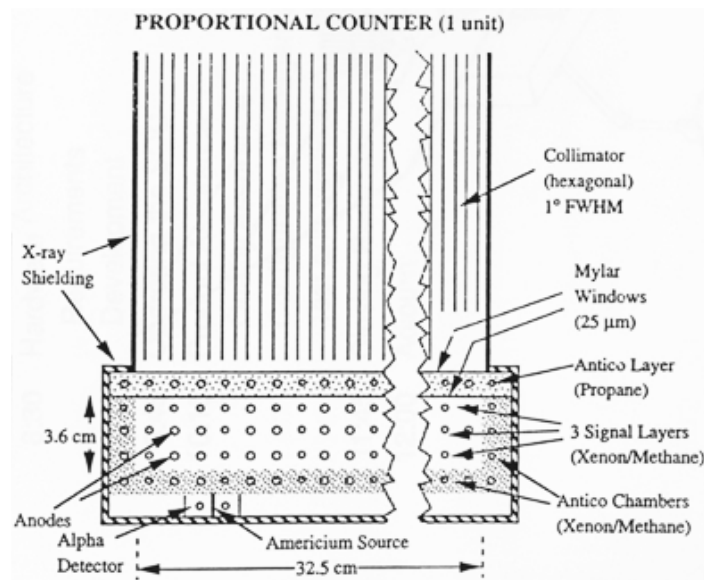


Figure 1.3 This Figure is a cross section of one proportional counter of the PCA. Figure reproduced from NASA website for RXTE

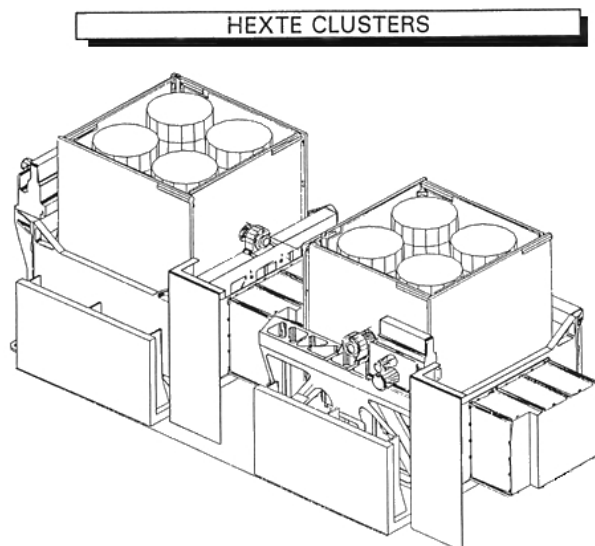


Figure 1.4 Figure shows the HEXTE cluster. Figure reproduced from NASA website for RXTE

1.6.2 High Energy X-ray Timing Experiment

HEXTE consists of eight phoswich scintillation detectors divided in two clusters, each containing four detectors. The detectors are NaI/CsI scintillators. The total collecting area for one cluster is 800 cm^2 . Figure 1.4 shows the HEXTE clusters and Figure 1.5 shows one phoswich. HEXTE has an energy resolution of 15% at 60 keV and a timing resolution of 8 microsecond. This instrument is very useful for extending the spectral studies of sources upto a higher energy of 150 keV. A source of 1 Crab will give a count rate of 350 counts/s per HEXTE cluster. Each cluster has a background count rate of 50 count/s.

1.6.3 All Sky Monitor

ASM consists of three wide-angle shadow cameras which are made of position-sensitive Xenon proportional counters with a total collecting area of 90 square cm. ASM assembly is shown in Figure 1.6 and Figure 1.7 shows one of the ASM shadow cameras. ASM operates

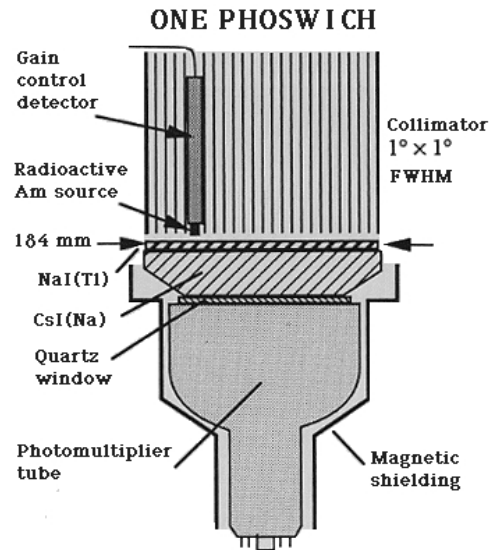


Figure 1.5 Figure shows one phoswich scintillator detector. Figure reproduced from NASA website for RXTE

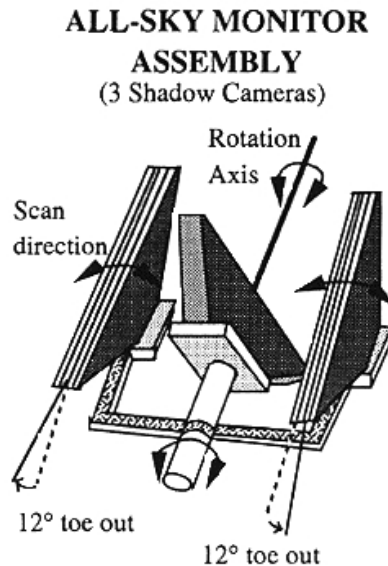


Figure 1.6 Schematic diagram shows the relative orientation of the SSCs as configured on the ASM. Figure reproduced from Levine et al. 1996

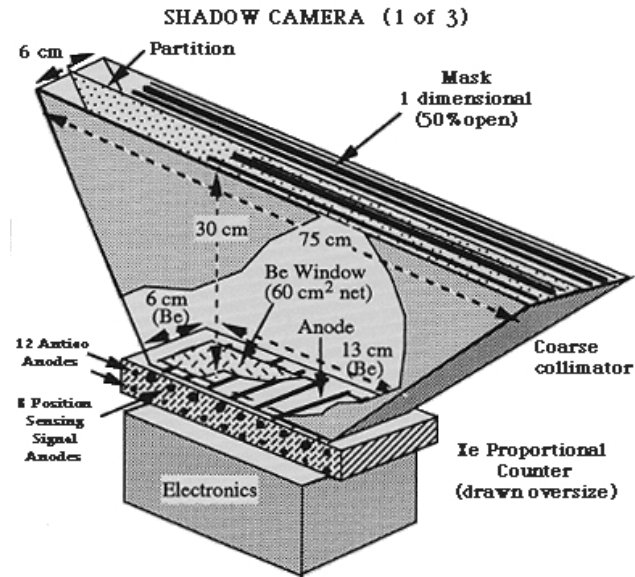


Figure 1.7 Figure shows one scanning camera of the ASM. Figure reproduced from NASA website for RXTE

in the energy range of 1.5-12 keV. It covers 80% of the sky every 90 minutes with a spatial resolution of $3' \times 15'$. Each of the three cameras has a field of view of 6×90 degrees. ASM has a sensitivity of 30 mCrab and is very useful in long term X-ray light curve variability studies.

This research has made use of data obtained from the Rossi X-ray Timing Explorer Web site (<http://rxte.gsfc.nasa.gov>). The RXTE Web site is a part of the High Energy Astrophysics Science Archive Research Center (HEASARC), provided by NASA's Goddard Space Flight Center.